PHYSICAL AND THERMAL CHARACTERISTICS OF EXPANDED FOAM GLASSES USING CRUDE GLYCEROL AS A FOAMING AGENT

Pat Sooksaen [1,2,*] and Penpisuth Thongyoug[3]

Received: November 18, 2022; Revised: December 27, 2022; Accepted: February 13, 2023

Abstract

Expanded foam glasses were fabricated from a clear color soda-lime silicate glass. Crude glycerol was used as an effective foaming agent which promoted small closed cell pores. This research studied the effect of crude glycerol content on the expanding characteristics and thermal properties. The expanding behavior relied on the thermal decomposition mechanism of the foaming agent as well as the sintereing temperature. Expanded foam glasses fabricated at 850°C showed uniform pore size compared to those fabricated at other temperatures (800°C and 900°C). Pore size of the synthesized foam glasses generally increased with increasing firing temperature. The evidence of black color in some areas for samples fabricated at 800°C occurred due to incomplete combustion of crude glycerol within the bulk structure. Samples produced at 850°C and 900°C showed white color shading associated with complete combustion of carbonaceous compound. Foam glasses sintered at 900°C showed structural distortion due to glass melting during the foaming process. Large holes or gaps within the structures occured due to the sweeping and combining of gas bubbles during sintering.

Keywords: Crude glycerol, Decomposition, Foam glass, Microstructure

Introduction

The concern over waste glass disposal has led to the study for recycling or fabricating into value added products. Expanded foam glass is one of the most promising materials that utilized waste glass in large quantity. It is a porous material where the solid phase is mainly a glass phase or crystallized glass phase filled with pores in which the pore cells can be of several micrometers to millimeters. The most promissing method for fabricating expanded foam glass is by mixing a fine glass powder with a pore-forming agent (or foaming agent) which can gennerate gas bubbles at elevated temperatures. (Wang *et al.*, 2018). During the heat treatment (or sintering) foaming agent releases gas or gases that form finely dispersed bubbles in the softened viscous glass (Petersen *et al.*, 2017). The expanding

[1] *Department of Materials Science and Engineering, Faculty of Engineering and Industrial Technology, Silpakorn University, Nakhon Pathom 73000 Thailand. E-mail: sooksaen_p@silpakorn.edu*
[2] *Center of Excellence for Petroleum, Petrochemicals and Advanced Materials, Chulalongkorn University, Bangkok, 10330, Thailand.*
[3] *Department of Industrial Engineering and Management, Faculty of Engineering and Industrial Technology, Silpakorn University, Nakhon Pathom 73000 Thailand.*
[*] *Corresponding author*

gas bubbles hence increase the volume of the bulk sample. Pore forming agents are mostly carbon based compounds which may lead to residues which will not go into the glass network. (Fernandes *et al.*, 2009; König *et al.*, 2016; Qu *et al.*, 2016). After sintering, the product is cooled slowly to avoid cracking due to thermal stress.

Expanded foam glass possesses unique and excellent properties such as lightweight, rigid, high in surface area, non-flammable, thermal and acoustic insulating, chemically inert, non-toxic and environmentally friendly (Kidalova *et al*., 2012; Zhang *et al.*, 2016; Souza *et al.*, 2017; Wei *et al.*, 2017). In construction, foam glass can be applied as a lightweight filler in concrete which will give advantages of lightweight, thremal insulation and low water penetrating characteristics (Bumanis *et al*., 2003; Bumanis *et al.*, 2013; Yu *et al*., 2016; Zhu *et al.*, 2016, Adhikary *et al.*, 2021). Foam glass also possesses high mechanical strength and thermal stability far better than polymeric foams. In the case of a fire, polymeric foams can be highly damaged with toxic gases released. (Šeputytė-Jucikė and Sinica, 2016) In contrast, foam glass is very resistant to flame due to the inorganic nature. Foam glass can also be applied in some specific applications such as catalyst support and microorganism-immobilized carriers for organic wastewater treatment (Chen *et al.*, 2020).

The objectives of this study were to understand the effect of the increase in crude glycerol content and the sintering temperature on the structure of foam glasses fabricated in an electric muffle furnace. Crude glycerol from biodiesel refinery plant was utilized as an effective foaming agent which released gas at elevated temperatures. The use of crude glycerol as a foaming agent for the production of foam glass was hardly found in the related literature. Sodium silicate was used as a binder and a fluxing agent in soda-lime based glass system.

Materials and Methods

The soda-lime silicate glass utilized in this study was obtained from consumable drink bottles. The glass composition was analyzed by X-ray Fluorescence Spectrometer WDXRF ZXS Primus, Rigaku, Japan) which gave the composition in wt% as 69.2 SiO_2 - 12.4Na_2O - 13.8 CaO - 2.4 MgO - 1.5 Al_2O_3 - 0.2 K_2O - 0.15 Fe_2O_3 - 0.02 P_2O_5. The glass was ball milled in 5 kg pot mill using alumina milling media in various sizes; 2, 3 and 4 mm diameter. The milling process was carried out for 12 h to give fine glass powder and sieved through a sieve shaker (Retsch AS200) to give particle size of < 120 μm.

Crude glycerol was supplied by Siam Absolute Chemical Co. Ltd. (Thailand) which consisted of 78 wt% glycerol. Other compounds given by the supplier were methanol (<10%), water (~10%) methly esters (<5%) and other impurities such as inorganic catalyst residues. Sodium silicate (or water glass) was supplied by Amarin Ceramics (Thailand). It was used as a binder to hold the mixture composition in place during the heating process and also acted as a fluxing agent in soda-lime silicate glass. The effect of sodium was to give non-bridging oxygens in [SiO_4] corner-sharing tetrahedra in soda-lime silicate glass structure (Hesky *et al.* 2015). Solvent A is proposed in this study which consisted of 50% crude glycerol and 50% sodium silicate by volume. This solvent system resulted in good foaming behavior at temperature range of 780-950°C which had been investigated previously by the authors (unpublished data).

The compositions for expanded foam glasses in this study are shown in Table 1 where the solvent system was incorporated in excess amount compared to 100% glass powder.

Table 1. The foam glass compositions

Foam Glass	Glass powder (g)	Solvent A (g) (excess)
FG1	100	4
FG2	100	6
FG3	100	8
FG4	100	10

Sample preparation was carried out by uniaxial pressing 15 g of the mixture into a pellet. The applied pressure was 10 MPa and the compacted sample had a diameter of 30 mm and ~15 mm thickness. The compacted pellets were heated in an electric furnace for the foaming process. A heating rate of 5°C/min was applied until maximum temperature for the foaming process was reached. The foaming was carried out at 800, 850 and 900°C, respectively with a holding time of 15 min at each temperature. After foaming, the sample was slowly cooled in the furnace to room temperature to avoid cracking.

A DSC technique was carried out on crude glycerol to investigate for the thermal degradation behavior. Dilatometric analysis on the soda-lime silicate glass (5 mm × 5 mm × 2 mm) was carried out using Netzsch DIL 402 dilatometer operated at the heating rate of 10°C/min to investigate for the glass transition temperature and the dilatometric softening temperature. Pore size distribution diagrams were constructed from the images taken

by a D90 Nikon digital camera and a Tescan Mira3 scanning electron microscope depending on the pore size range. A number of at least 200 pores was chosen from the image for the calculation by line interception method. For SEM analysis, gold sputtering was applied to reduce charging effect caused by high porosity of foam glass samples. In addition, X-ray diffraction was carried out to analyze for the phases present in the fabricated foam glasses. A Shimadzu D6100 X-ray diffractometer with CuK_α radiation was used to collect the data at a scan speed of 5°/min and a step size of 0.02° 2θ.

Results and Discussion

Crude glycerol in Figure 1 exhibited a wide temperature range of thermal decomposition (Dou *et al.*, 2009). The highly endothermic peak at 306°C in Figure 1 was responsible for decomposition of glycerol and hydrated salts in crude glycerol. The residues (impurities such as the fatty acid methyl esters) of the main decomposition are much harder to eliminate via thermal which means that crude glycerol pyrolysis. An exothermic peak at 623°C was an unknown reaction but could be related to the change into more stable compound during heating. At temperature above 780°C, thermal cracking reactions (endothermic) of coke and ash were predominant giving CO_2 and CO. The decomposition phases were attributed to cracking of fatty acid methyl esters and pyrolysis residues (Hemings *et al.*, 2012). However, due to high oxygen content it is very difficult to understand the characteristics of pyrolysis of the crude glycerol from the biodiesel production process.

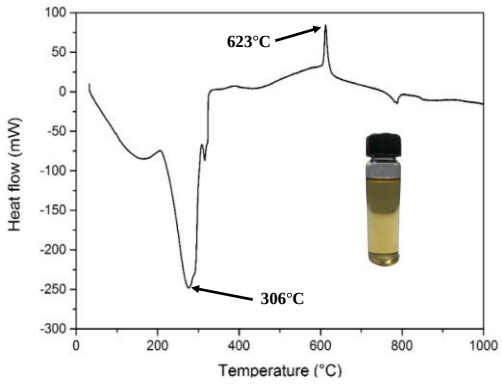

Figure 1. DSC analysis of crude glycerol

Dilatomtric analysis of the soda lime silicate glass in Figure 2 shows a linear relationship from room temperature to around 540°C indicting a characteristic of a rigid solid glass with a constant thermal expansion coefficient. The glass transition, T_g was observed at the first slope change at 543°C and the dilatometric softening point occurred at 595°C after which the dilatometric slope became negative indicating softened behavior of the glass. In this study fine glass powder at high temperatures became low in viscosity and the particles partially melted and formed continuous neck encapsulating the pore-forming agent. The decomposition of pore-forming agent occurred at the sintering temperature and released high pressure gas or gases into a viscous glass melt.

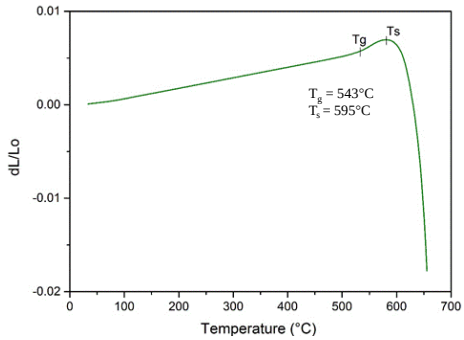

Figure 2. Dilatomtric analysis of the soda lime silicate glass

Foam glass samples FG1-FG4 sintered at 800°C (Figure 3) showed a clear evidence non-uniform pore size distribution and thick pore walls under visual inspection. The glass viscosity at this processing temperature may have been too high such that the gas pressure was not able to exert evenly on the highly viscous glass. At this sintering temperature, there was an evidence of black color in most areas caused by incomplete combustion of carbon containing compounds from crude glycerol. Foam glasses sintered at 850°C also showed a more uniform pore size distribution and thinner pore walls under visual inspection. All samples showed more white color shading which can be clearly seen in Figure 4. Although some white spot areas were still present from incomplete combustion of the foaming agent. At this temperature, the pores were small and exhibited good roundness within the closed cell structure. In samples sintered at 900°C, pores were still in spherical shape and showed white color shading throughout the bulk structure (Figure 5). FG3 and FG4 samples showed structural distortion which was possibly caused by higher sintering temperature. In addition, at this sintering temperature pores increased in size and connected to each other and grew by the sweeping and combining of gas bubbles. This was evident in FG4

sample which showed a higher fluxing effect from sodium silicate and a higher gas pressure could have produced (from higher amount of crude glycerol) which exerted on the less viscous glass. There was an evidence of pore coalescence that occurred in some areas leading larger pores or gaps. Bulk structure collapsing at its own weight was also observed at this sintering temperature which may have been due to reduced glass viscosity. This then resulted in sample shrinkage after sintering.

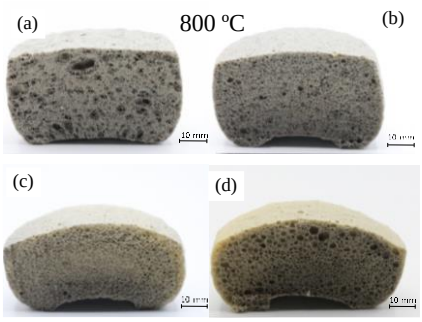

Figure 3. Expanded foam glasses heated at 800°C (a) FG1 (b) FG2, (c) FG3 and (d) FG4 Scale bar = 10 mm

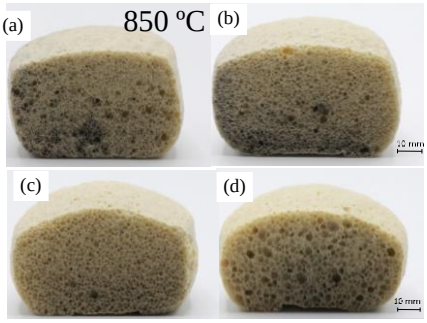

Figure 4. Expanded foam glasses heated at 850°C (a) FG1 (b) FG2, (c) FG3 and (d) FG4 Scale bar = 10 mm

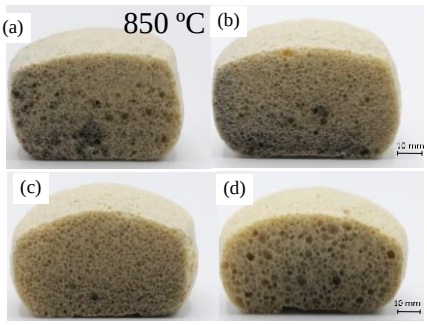

Figure 5. Expanded foam glasses heated at 900°C (a) FG1 (b) FG2, (c) FG3 and (d) FG4 Scale bar = 10 mm

As far as the size of bulk foam glass samples was concerned, the % linear expansion was calculated from side view (left to right) and each sample was measured an averaged from five positions. The data in Figure 6 showed a general trend of increasing in % linear expansion when the amount of solvent A incorporated in the composition was increased from 4 to 10%. With 4% solvent addition, the linear expansion varied in the range of 51-73% where at 10% solvent addition, the linear expansion greatly increased which varied in the range of 94-112%. Focusing on the sintering temperature, it was evident that sintering at 850°C resulted in higher % expansion as compared to 800 and 900°C. This behavior has been discussed earlier in the concept of glass viscosity and gas pressure in the sintering temperature range of 800 - 900°C.

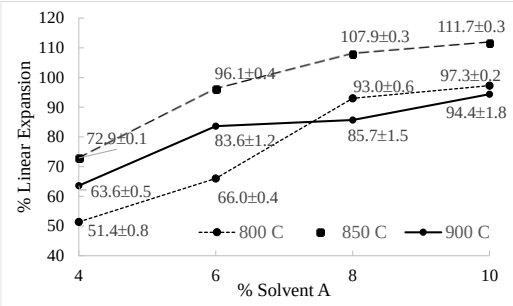

Figure 6. % Linear expansion of expanded foam glasses fabricated at 800, 850 and 900°C for FG1 - FG4

The magnified images of pore structures were obtained from a field emission electron microscope or a digital camera depending on the pore sizes which can be best observed and measured. The pore size scale on the x-axis can be separated into many ranges on an SEM image whereas for the images taken from a digital camera it was difficult to count for the number of pores so less pore size ranges were measured.

For FG1 with 4% solvent addition, pores were very small therefore an SEM was required to magnify the porous structure. Figure 7 showed pore size distribution of expanded foam glasses FG1 - FG4 (4, 6, 8, 10% solvent A) fabricated at 800°C. Closed pores were observed throughout the structure in all four compositions. In FG1 sample, the pore distribution was in the range of 100-500 μm. Most of the pores were in the size range of 100-200 μm which accounted for about 72% total volume. Increasing the percentage of solvent addition resulted in a higher value of pore size and the pore size distribution range shifted to the right

hand side. FG2 sample showed that 65% of the total pore volume had the size of 200 μm. For FG3, most of the pores (~51%) had the size of 500 μm and for FG4 most of the pores were in the range of 1000-1500 μm (~68%). When considering pore size distribution of expanded foam glasses FG1 - FG4 (4, 6, 8, 10% solvent A) fabricated at 900°C (Figure 8). It can be clearly seen that the size ranges increased to higher values that those in the samples fabricated at 800°C. In FG1 sample, most of the pores (~53%) had the pore size in the range of 100-300 μm and the size range of 400-600 μm was accounted for about 30%. FG2 sample showed that ~72% of the total pores had the size of 1000 μm and ~25% had the size of 2000. The distribution shifted to the right for FG3 sμm ample to give ~60% total pore with 1000 μm and ~35% with 2000 μm. Pore size in FG4 samples increased.

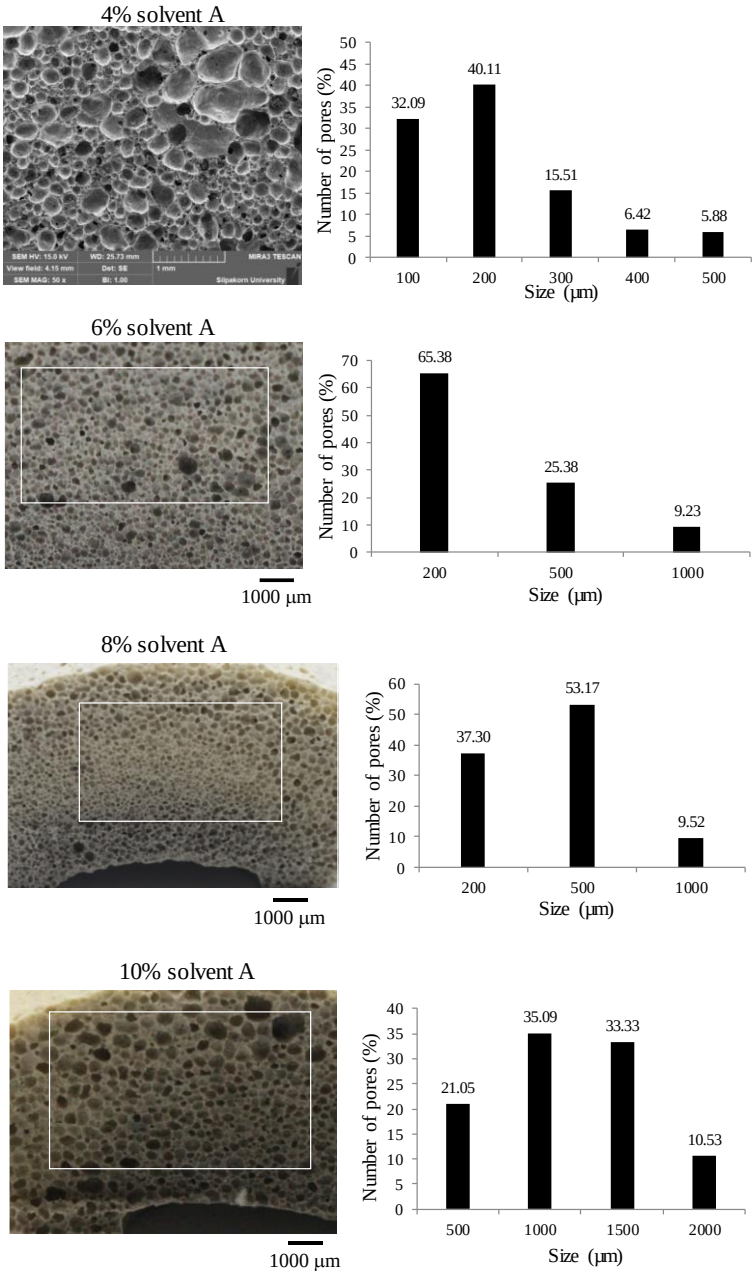

Figure 7. Pore size distribution of expanded foam glasses FG1 - FG4 (4, 6, 8, 10% solvent A) fabricated at 800°C

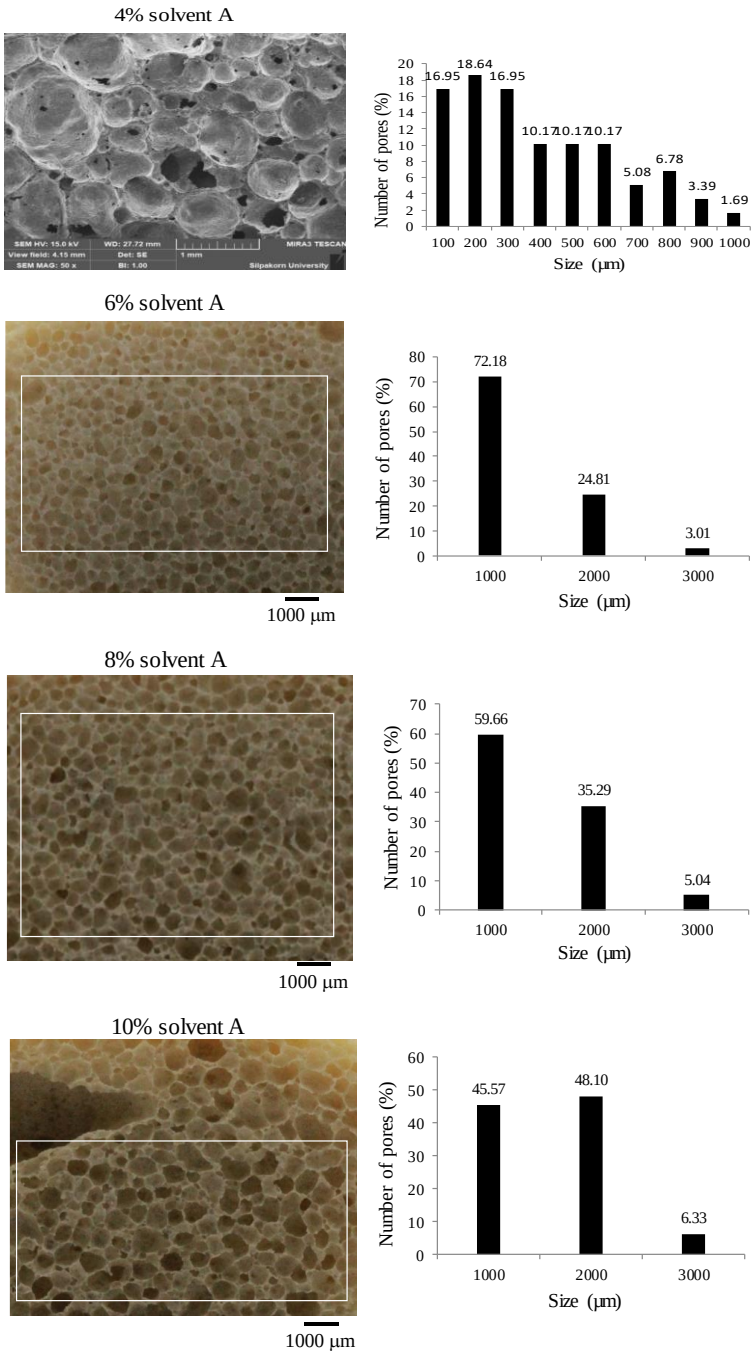

Figure 8. Pore size distribution of expanded foam glasses FG1 - FG4 (4, 6, 8, 10% solvent A) fabricated at 900°C

As far as the phases in the fabricated foam glasses were concerned (Figure 9), it can be seen that at 800°C all the foam glass compositions gave broad diffraction which is a characteristic of amorphous glass. Increasing the sintering temperature to 850°C and above resulted in the crystallization of crystalline phases. These phases appeared in low intensities in the amorphous broad diffraction background. The crystalline phases were analyzed as quartz (Q: JCPDS #01-083-0539), cristobalite (CB: JCPDS #00-039-1425) and devitrite (D: JCPDS #00-023-0671) - $Na_2Ca_3Si_6O_{16}$. In this study the effect of crystallization on the foaming behavior has not been investigated and it

requires a number of characterization techniques to fully understand such behavior. In some literature there were evidences for the effect of crystallization which resisted the foaming process which then led to low expansion of foam glass or foam glass-ceramic. Figure 10 showed SEM images of FG4 samples which confirmed the evidence of crystalline phases of different morphologies. It can be seen from higher magnification images in figure 10b that the higher the sintering temperature, the greater the crystalline content. The samples had been prepared by etching in 5% HF acid for 30-60 s to remove silica based glasses so that crystalline phases can be better observed. Sintering at 800°C showed smooth background presumably the residual glassy phase after etching.

Thermal Conductivity (K) and thermal resistivity (R) were evaluated in this study following ASTM C518 using HC074-200 EKO Instruments. The uncertainty of the test was ±0.0003 W/m·K. The test results are shown in Table 2. Foam glass samples sintered at 850°C were chosen for the evaluation. Overall, the K and R values of FG1-FG4 were very close; K 0.27-0.32 W/m.K and R 0.03-0.04 W/m^2.K. This indicated excellent thermal insulating characteristics of the fabricated foam glasses. It was clearly seen that the K value decreased gradually (as opposed to a slight increase in R value) from FG1 to FG4, which confirmed a well correlation to larger pore sizes in foam glass samples fabricated with a higher amount of foaming agent.

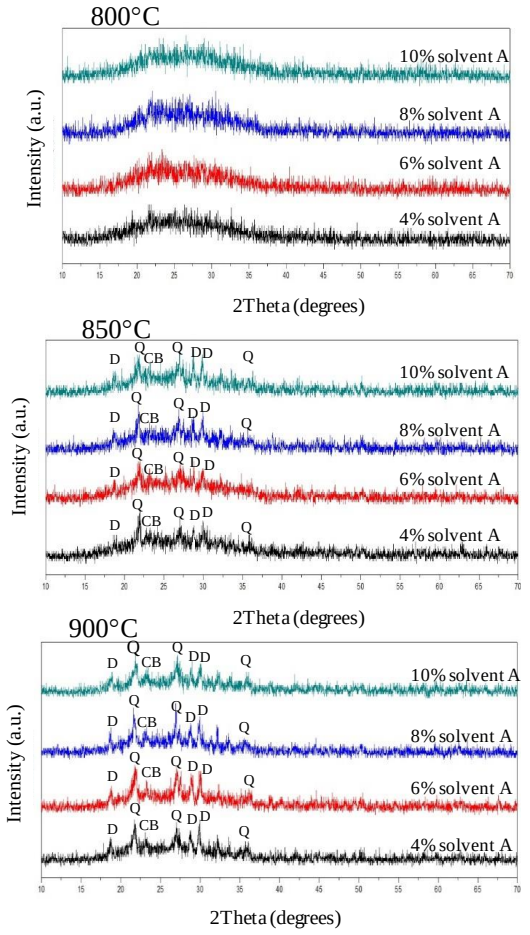

Figure 9. X-ray dittraction analysis of expanded foam glasses FGI-FG4 (4, 6, 8, 10% solvent A) Fabricated at 800, 850 and 900°C

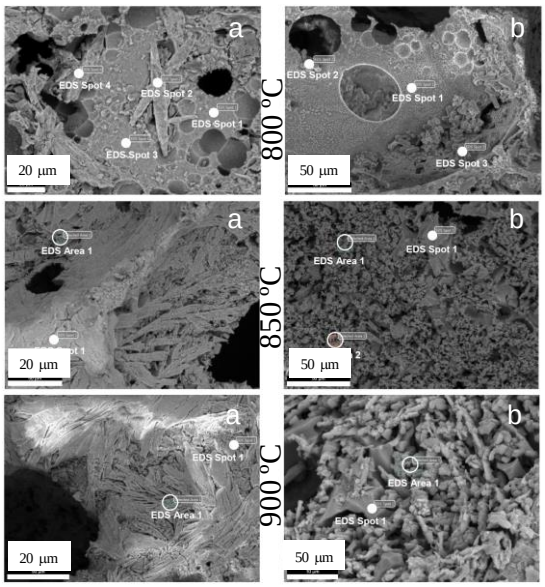

Figure 10. SEM images of FG4 samples sintered at 800, 850 and 900°C

Table 2. Thermal conductivity and resistivity of foam glasses fabricated at 850°C

Foam glass sample	Thermal conductivity/resistivity		
	Thicness (m)	K-Value (W/m K)	R-Value (m^2 K/W)
FG1	0.0100±0.0005	0.30330±0.0003	0.0417
FG2	0.0097±0.0005	0.3202±0.0003	0.0314
FG3	0.0100±0.0005	0.2987±0.0003	0.0325
FG4	0.0126±0.0005	0.2712±0.0003	0.0369

Conclusions

Crude glycerol promoted the foaming behavior which resulted in small spherical closed pores. The higher the amount of crude glycerol and the fluxing agent in the composition, the easier the foaming process. The samples expanded more and lager pores were obtained. Sintering at 850°C and above showed white color shading which was related to the complete combustion of carbon containing compounds in crude glycerol.

Pore size also increased with increasing sintering temperature. Foam glasses sintered at 900°C showed some structure distortion due to glass melting and bulk structure slightly collapsed during the foaming process. It was more evident in the composition containing higher amount of solvent. Also, large gaps or holes in the samples fabricated at 900°C were caused by the sweeping and combining of gas bubbles within the samples.

Acknowledgements

This research is financially supported by Thailand Science Research and Innovation (TSRI) National Science, Research and Innovation Fund (NSRF) (Fiscal Year 2022). We also thank the department of Materials Science and Engineering, Faculty of Engineering and Industrial Technology, Silpakorn University for research facilities, and previous undergradute students; Tanin Unnapan, Suphahud Pintasiri and Puttarapapa Meetongpun for some collected data.

References

Adhikary, S.K., Ashish, D.K. and Rudžionis, Ž. (2021) Expanded glass as light-weight aggregate in concrete - A review. Journal of Cleaner Production, 313(1):127,848. https://doi.org/10.1016/j.jclepro.2021.127848

Bumanis, G., Bajare, D. and Korjakins, A. (2003). Mechanical and Thermal Properties of Lightweight Concrete Made from Expanded Glass. Journal of Sustainable Architecture and Civil Engineering, 2(3):19-25. https://doi.org/10.5755/j01.sace.2.3.2790

Bumanis, G., Bajare, D. Locs, J. and Korjakins, A. (2013). Alkali-silica reactivity of foam glass granules in structure of lightweight concrete. Construction and building materials, 47:274-281

Chen, N.H., Zhang, S.H., Pan, X.Y., Zhou, S., and Zhao, M. (2020). Foaming mechanism and optimal process conditions of foamed glass based on thermal analysis. Journal of Porous Materials, 27:621-626 https://doi.org/10.1007/s10934-020-00864-6

Dou, B., Dupont, V., Williams, P.T., Chen, H., and Ding, Y. (2009). Thermogravimetric kinetics of crude glycerol. Bioresour. Technol., 100(9):2613. https://doi.org/10.1016/j.biortech.2008.11.037

Fernandes, H., Tulyaganov, D. and Ferreira, J. (2009). Preparation and characterization of foams from sheet glass and fly ash using carbonates as foaming agents. Ceramics International, 35(1):229-235. https://doi.org/10.1016/j.ceramint.2007.10.019

Hemings, E.B., Cavallotti, C., Cuoci, A., Faravelli, T. and Ranzi, E. (2012). A detailed kinetic study of pyrolysis and oxidation of glycerol (propane-1, 2, 3-triol). Combustion Science and Technology, 184(7-8):1,164-1,178. https://doi.org/10.1080/00102202.2012.664006

Hesky, D., Aneziris, C.G., Gross, U. and Horn, A. (2015). Water and waterglass mixtures for foam glass production. Ceramics International, 41(10):12,604-12,613. https://doi.org/10.1016/j.ceramint.2015.06.088

Kidalova, L., Stevulova, N., Terpakova, E., Sicakova, A. (2012). Utilization of alternative materials in lightweight composites. Journal of Cleaner Production, 34:116-119. https://doi.org/10.1016/j.jclepro.2012.01.031

König, J., Petersen, R.R., and Yue, Y. (2016). Influence of the glass particle size on the foaming process and physical characteristics of foam glasses. Journal of Non-Crystalline Solids, 447:190-197. https://doi.org/10.1016/j.jnoncrysol.2016.05.021

Petersen, R.R., König, J., and Yue, Y. (2017). The viscosity window of the silicate glass foam production. Journal of Non-Crystalline Solids, 456:49-54. https://doi.org/10.1016/j.jnoncrysol.2016.10.041

Qu, Y.N., Xu, J., Su, Z.G., Ma, N., Zhang, X.Y., Xi, X.Q., and Yang, J.L. (2016). Lightweight and high-strength glass foams prepared by a novel green spheres hollowing technique. Ceramics International, 42(2):2,370-2,377 https://doi.org/10.1016/j.ceramint.2015.10.034

Šeputytė-Jucikė, J. and Sinica, M. (2016). The effect of expanded glass and polystyrene waste on the properties of lightweight aggregate concrete. Engineering Structures and Technologies, 8(1):31-40. https://doi.org/10.3846/2029882X.2016.1162671

Souza, M.T., Oliveira Maia, B.G., Teixeira, L.B., Oliveira, K.G., Teixeira, A., and Oliveira, A.P.N. (2017). Glass foams produced from glass bottles and eggshell wastes. Process Safety and Environmental Protection, 111: 60-64. https://doi.org/10.1016/j.psep.2017.06.011

Wang, H., Chen, Z.W., Ji, R., Liu, L.L., Wang, X.D. (2018). Integrated utilization of high alumina fly ash for synthesis of foam glass ceramic. Ceram. Int. 44: 13681-13688 https://doi.org/10.1016/j.ceramint.2018.04.207

Wei, Y.L.,Cheng, S.H., Ou, K.T., Kuo, P.J., Chung, T.H., and Xie, X.Q. (2017). Effect of calcium compounds on lightweight aggregates prepared by firing a mixture of coal fly ash and waste glass. Ceramics International, 43(17): 15573-15579 https://doi.org/10.1016/j.ceramint.2017.08.110

Yu, R., Van Onna, D.V., Spiesz, P., Yu, Q.L., Brouwers, H.J.H. (2016). Development of Ultra-Lightweight Fibre Reinforced Concrete applying expanded waste glass. Journal of Cleaner Production, 112, Part 1: 690-701. https://doi.org/10.1016/j.jclepro.2015.07.082

Zhang, Q., He, F., Qiao, Y., Mei, S.X., Jin, M.F. and Xie, J. (2016). Preparation of high strength glass ceramic foams from waste cathode ray tube and germanium tailings. Construction and Building Materials, 111:105-110. https://doi.org/10.1016/j.conbuildmat.2016.01.036

Zhu, M., Ji, R., Li, Z.M., Wang, H., Liu, L.L. and Zhang, Z. (2016). Preparation of glass ceramic foams for thermal insulation applications from coal fly ash and waste glass. Construction and Building Materials, 112:398-405. https://doi.org/10.1016/j.conbuildmat.2016.02.183